arXiv:1607.02807v3 [cond-mat.supr-con] 22 Jul 2016

Hall Effect in the Abrikosov Lattice of Type-II Superconductors

Wataru Kohno, Hikaru Ueki, and Takafumi Kita

Department of Physics, Hokkaido University, Sapporo 060-0810, Japan

We study vortex charging caused by the Lorentz force on supercurrent based on the augmented quasiclassical equations of superconductivity. Our numerical study on an s-wave vortex lattice in the range $H_{c1} < H < H_{c2}$ reveals that each vortex core with a single flux quantum also accumulates charge due to the circulating supercurrent and has a Hall voltage across the core. The field dependence of the charge density at the core center is well described by $\rho(\mathbf{0}) \propto H(H_{c2}-H)$ with a peak near $H_{c2}/2$ originating from competition between the increasing magnetic field and the decreasing pair potential. The peak value of the accumulated charge in a core region of radius $0.5\xi_0$ is estimated to be about $\eta\Delta_0/(k_F\xi_0)\times|e|$ C per $\Delta z = 10$ Å along the flux line at low temperatures, where $\eta \equiv \pi\epsilon_0\Delta z/|e|^2 = 1.09\times10^{18}$ J^{-1} with $e<0$ the charge of an electron, Δ_0 the energy gap at $T=0$, k_F the Fermi wave number, and ξ_0 the coherence length at $T=0$.

The Lorentz force on electric currents flowing in magnetic fields has a unique component perpendicular to both the current and field. It generally induces charge redistribution before recovering a steady state to produce a Hall voltage that eventually brings about force balance along the transverse direction. Extensive studies have been performed over the last few decades on this *Hall effect*[1] in metals and semiconductors, especially on the quantum Hall effect in two dimensions.[2]

In contrast, we still have little understanding of the phenomena in superconductors. This is because the force on supercurrent itself may easily be overlooked in the presence of the predominant diamagnetic effect by supercurrent obeying Ampère's law. Indeed, the Lorentz force is missing from the Ginzburg–Landau[3] and Eilenberger[4] equations that have been used extensively in the literature,[5–7] and can only be reproduced microscopically as a next-to-leading-order contribution in the expansion of the Gor'kov equations in terms of the quasiclassical parameter $\delta \equiv 1/k_F\xi_0$.[8,9] Hence, the physics of the Lorentz force in superconductors remains mostly theoretically unexplored.

This Hall effect in superconductors may be divided into two categories: one in equilibrium with persistent currents[9–14] and the other in nonequilibrium situations with the motion of vortices and dissipation.[6,15–18] The first one is inherent to superconductors and easier to handle but nevertheless has not been paid much attention in the literature. We here focus on this first category and study vortex charging in type-II superconductors as a function of the magnetic field based on the augmented quasiclassical equations of superconductivity.[8,9]

It has been previously shown that charge accumulation due to the Lorentz force occurs in equilibrium near edges in the Meissner state[10–14] and also around the core of an isolated vortex slightly above the lower critical field H_{c1}.[9] With these results and noting that the Lorentz force is proportional to the flux density B, we expect an enhancement of the charging in finite magnetic fields. To clarify this point, we here consider an s-wave vortex lattice and calculate its charge distribution numerically as a function of the magnetic field from H_{c1} up to the upper critical field H_{c2} at various temperatures. It is thereby shown that the charge density at the vortex center has a strong field dependence with a peak around $H_{c2}/2$ whose value is 10–100 times larger than that of the isolated vortex. This field dependence is characteristic of charging by the Lorentz force making it experimentally distinguishable from other possible mechanisms for vortex-core charging.[19–25] In this context, Khomskii and Freimuth[19] and Feigel'man and coworkers[20,21] proposed different mechanisms by regarding the core region as the normal state and considering its chemical-potential difference from the surroundings.[19–21] However, the resulting charge accumulation, if any, should decrease monotonically as H is increased because of the decreasing pair potential.

We now study the charge and electric-field distributions due to the Lorentz force in the vortex lattice of a clean s-wave type-II superconductor. To this end, we use the augmented quasiclassical equations in the Matsubara formalism.[9] As shown in Ref. 9, they can be decoupled into an electric-field equation plus the standard Eilenberger equations through an expansion in terms of the dimensionless quasiclassical parameter $\delta \ll 1$. The Eilenberger equations are reproduced in this procedure by collecting terms of $O(1)$ in the expansion. They are given by[6,7,26,27]

$$\omega_n f + \frac{1}{2}\hbar\boldsymbol{v}_F\cdot\left(\boldsymbol{\nabla} - i\frac{2e\boldsymbol{A}}{\hbar}\right)f = \Delta g, \tag{1a}$$

$$\Delta = g_0\pi k_B T\sum_{n=-\infty}^{\infty}\langle f\rangle_F, \tag{1b}$$

$$\boldsymbol{\nabla}\times\boldsymbol{\nabla}\times\boldsymbol{A} = -i2\pi e\mu_0 N(0)k_B T\sum_{n=-\infty}^{\infty}\langle\boldsymbol{v}_F g\rangle_F, \tag{1c}$$

with the normalization condition $g = \mathrm{sgn}(\omega_n)\left(1-f\bar{f}\right)^{1/2}$. Here $\omega_n \equiv (2n+1)\pi k_B T$ ($n = 0, \pm1, \cdots$) with k_B and T denoting the Boltzmann constant and temperature, $f =$

$f(\omega_n, \boldsymbol{p}_\mathrm{F}, \boldsymbol{r})$ is the anomalous quasiclassical Green's function and $f \equiv f^*(\omega_n, -\boldsymbol{p}_\mathrm{F}, \boldsymbol{r})$, $\boldsymbol{p}_\mathrm{F}$ and $\boldsymbol{v}_\mathrm{F}$ are the Fermi momentum and Fermi velocity, and $e < 0$ is the charge of an electron, respectively. Equations (1b) and (1c) are the self-consistency equation for the pair potential $\Delta(\boldsymbol{r})$ and Maxwell's equation (Ampère's law) for the vector potential $\boldsymbol{A}(\boldsymbol{r})$, respectively, where $g_0 \ll 1$ is a dimensionless coupling constant responsible for the Cooper pairing, $\langle \cdots \rangle_\mathrm{F}$ denotes the Fermi surface average normalized as $\langle 1 \rangle_\mathrm{F} = 1$, $N(0)$ is the normal density of states per spin and unit volume at the Fermi energy, and μ_0 is the vacuum permeability.

The Lorentz force emerges as a correction of $O(\delta)$, which is shown to induce an electric field $\boldsymbol{E}$ that obeys[9,10]

$$(-\lambda_\mathrm{TF}^2 \boldsymbol{\nabla}^2 + 1)\boldsymbol{E} = -i\pi k_\mathrm{B} T \boldsymbol{B} \times \sum_{n=-\infty}^{\infty} \left\langle \frac{\partial g}{\partial \boldsymbol{p}_\mathrm{F}} \right\rangle_\mathrm{F}, \qquad (2)$$

where $\lambda_\mathrm{TF} \equiv \sqrt{\epsilon_0/2e^2N(0)}$ is the Thomas–Fermi screening length with ϵ_0 the vacuum permittivity. Note that the source term on the right-hand side of Eq. (2) is given by the solutions g and $\boldsymbol{B} = \boldsymbol{\nabla} \times \boldsymbol{A}$ from Eq. (1). Hence, we can calculate electric fields generated by the Hall effect in various external circumstances based on the solutions of Eq. (1).

Here, we use Eq. (1) to construct vortex-lattice solutions of an s-wave pairing on a two-dimensional isotropic Fermi surface, which is perpendicular to the magnetic field. The corresponding vector potential is expressible in terms of the average flux density $\boldsymbol{B} = (0, 0, \bar{B})$ as $\boldsymbol{A}(\boldsymbol{r}) = (\bar{\boldsymbol{B}} \times \boldsymbol{r})/2 + \tilde{\boldsymbol{A}}(\boldsymbol{r})$,[7,28] where $\tilde{\boldsymbol{A}}$ describes the spatial variation of the flux density. Functions $\tilde{\boldsymbol{A}}$ and Δ for the triangular lattice obey the following periodic boundary conditions:[28–30]

$$\tilde{\boldsymbol{A}}(\boldsymbol{r} + \boldsymbol{R}) = \tilde{\boldsymbol{A}}(\boldsymbol{r}), \qquad (3a)$$

$$\Delta(\boldsymbol{r} + \boldsymbol{R}) = \Delta(\boldsymbol{r}) \exp\left[i\frac{|e|}{\hbar} \bar{\boldsymbol{B}} \cdot (\boldsymbol{r} \times \boldsymbol{R}) + i\pi n_1 n_2 \right], \qquad (3b)$$

where $\boldsymbol{R} = n_1\boldsymbol{a}_1 + n_2\boldsymbol{a}_2$ with n_1 and n_2 denoting integers, and $\boldsymbol{a}_1 = a_2(\sqrt{3}/2, 1/2, 0)$ and $\boldsymbol{a}_2 = a_2(0, 1, 0)$ are the basic vectors of the triangular lattice with length a_2 determined by the flux-quantization condition $(\boldsymbol{a}_1 \times \boldsymbol{a}_2) \cdot \bar{\boldsymbol{B}} = h/2|e|$.

Equation (1) with the boundary condition in Eq. (3) can be solved iteratively for a given set of $(T, \bar{B})$. It is convenient for this purpose to transform Eq. (1a) into the Riccati form.[7,31,32] In the first iteration, we substitute the trial functions

$$\Delta(\boldsymbol{r}) = \Delta_T \sqrt{1 - \frac{\bar{B}}{B_{c2}}} \Psi_\mathrm{sym}(\boldsymbol{r}), \qquad \tilde{\boldsymbol{A}}(\boldsymbol{r}) = \boldsymbol{0} \qquad (4)$$

into the Riccati form of Eq. (1a), where Δ_T is the energy gap at $\bar{B} = 0$, $B_{c2} = \mu_0 H_{c2}$ is the upper critical field obtained by applying Helfand-Werthamer theory[33,34] to the present cylindrical Fermi surface, and Ψ_sym is Abrikosov's solution of the linearized Ginzburg–Landau equations in a symmetric gauge without prefactors.[7,28] We then apply the method of solving Eq. (1a) for an isolated vortex[7] to a circle of radius R ($\gg a_2$) with many unit cells, focusing our attention to a single unit cell in the central region. To be more specific, we start the integration from $f = 0$ on the boundary with the hope that it will produce the relevant periodic solution in a unit cell far from the boundary because of the periodicity of the source term in Eq. (4). The resulting f in the unit cell is subsequently used to update Δ and $\tilde{\boldsymbol{A}}$ by Eqs. (1b) and (1c), which are then connected outside by Eq. (3) and substituted into Eq. (1a) for the next iteration. The convergence of the iteration can be checked by monitoring the free energy[4,30,35] of the unit cell. We confirmed that the free energy decreases as the iteration proceeds, which was stopped when the relative difference between the old and new free energies decreased to below 5.0×10^{-4}. We also checked that choosing $R \gtrsim 4a_2$ brings about excellent convergence with respect to R .

Functions g and $\boldsymbol{B} = \boldsymbol{\nabla} \times \boldsymbol{A}$ thereby obtained are used to construct the source term on the right-hand side of Eq. (2). The differentiation with respect to $\boldsymbol{p}_\mathrm{F}$ can be performed numerically without difficulties for the present cylindrical Fermi surface. Equation (2) with the source term is then solved by the finite-difference method[36] to obtain $\boldsymbol{E}(\boldsymbol{r})$ in the vortex lattice, which is substituted into Gauss' law $\rho(\boldsymbol{r}) = \epsilon_0 \boldsymbol{\nabla} \cdot \boldsymbol{E}$ to find the charge distribution. We checked that the charge neutrality within the unit cell is satisfied.

Our results below were obtained for $\delta \equiv 1/k_\mathrm{F}\xi_0 = 0.001$, $\lambda_\mathrm{TF}/\xi_0 = 0.001$, and $\lambda_\mathrm{L}/\xi_0 = 5.0$ unless stated otherwise, where $\xi_0 \equiv \hbar v_\mathrm{F}/\Delta_0$ and $\lambda_\mathrm{L} \equiv \sqrt{\hbar/\mu_0\Delta_0\xi_0 e^2 N(0) v_\mathrm{F}}$ are the coherence length and London penetration depth, respectively, defined in terms of the zero-temperature energy gap Δ_0 at $H = 0$. The temperature and charge density were normalized by the superconducting transition temperature T_c at $H = 0$ and $\rho_0 \equiv \Delta_0\epsilon_0/|e|\xi_0^2$, respectively.

Figures 1 and 2 show spatial variations of the charge density around a vortex core at $T/T_\mathrm{c} = 0.2$ calculated for $\bar{B}/B_{c2} = 0.073$ and 0.51, respectively. The charge in Fig. 1 is distributed isotropically with a conspicuous peak at the core center, indicating that this vortex in a low magnetic field is almost isolated. In contrast, the distribution at $\bar{B}/B_{c2} = 0.51$ strongly reflects the triangular symmetry of densely packed vortices. Moreover, we observe that the peak height at the core center is enhanced by an order of magnitude from the case of $\bar{B}/B_{c2} = 0.073$.

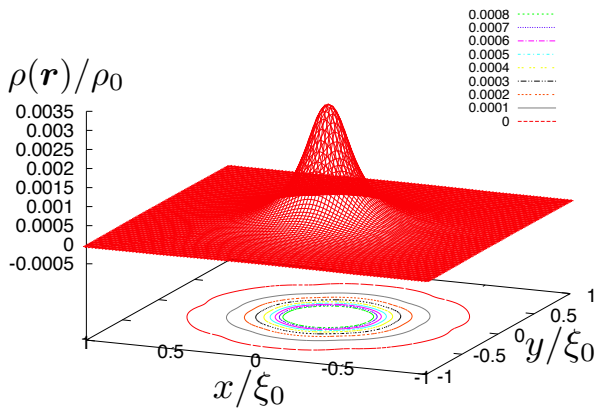

Fig. 1. (Color online) Charge density $\rho(\boldsymbol{r})/\rho_0$ in the core region $-1 \le x/\xi_0 \le 1$ for $\bar{B}/B_{c2} = 0.073$ at $T/T_\mathrm{c} = 0.2$, where $a_2 = 3.81\xi_0$.

Figure 3 shows the field dependence of the charge density $\rho(\mathbf{0})$ at the vortex center for $T/T_c = 0.2$ and 0.5. In both cases, $\rho(\mathbf{0})$ initially increases as the magnetic field is increased, reaches its maximum around $B_{c2}/2$, and decreases thereafter towards zero at B_{c2}. The initial increase can be attributed to the factor $\boldsymbol{B}$ in Eq. (2), whereas the latter decrease is due to the factor $\langle \partial g/\partial \boldsymbol{p}_F \rangle_F$, which decreases with decreasing pair potential. We found that the maximum value of $\rho(\mathbf{0})$ near $B_{c2}/2$ can be about 10–10^2 times larger than the peak value ρ_{single} at H_{c1} obtained by solving Eqs. (1) and (2) for an isolated vortex. Thus, vortex charging due to the Lorentz force has a strong field dependence with a peak and can be enhanced substantially from the value for an isolated vortex. This is the main finding of the present study.

This field dependence of the vortex-core charge can also be reproduced analytically near T_c. In this region, it is possible to expand the quasiclassical Green's functions (f, g) in Δ by regarding the gradient operator as $O(|\Delta|^1)$ and retaining terms

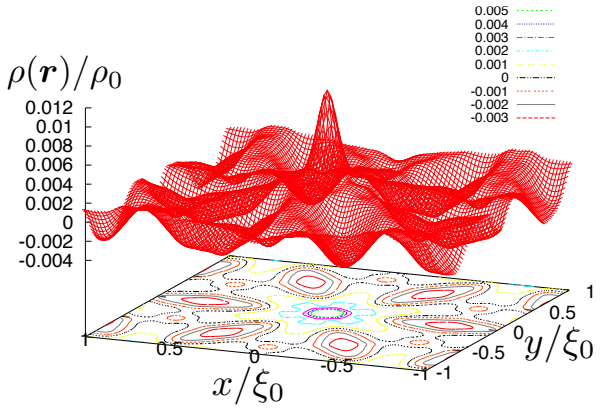

Fig. 2. (Color online) Charge density $\rho(\boldsymbol{r})/\rho_0$ in the core region $-1 \le x/\xi_0 \le 1$ for $\bar{B}/B_{c2} = 0.51$ at $T/T_c = 0.2$, where $a_2 = 1.44\xi_0$.

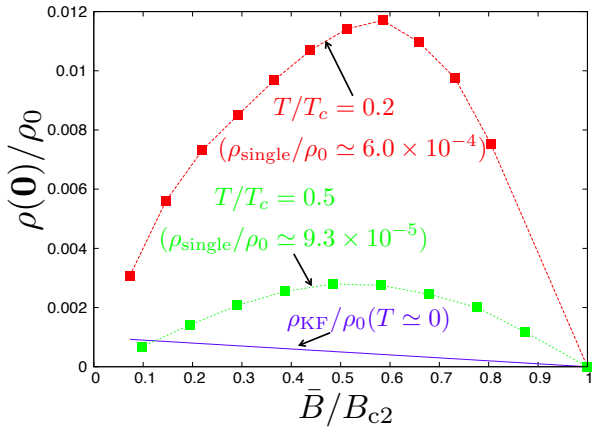

Fig. 3. (Color online) Normalized charge density at the vortex center, $\rho(\mathbf{0})/\rho_0$, as a function of magnetic field calculated for $T/T_c = 0.2$ (red line) and $T/T_c = 0.5$ (green line). The field dependence of ρ_{KF}/ρ_0 obtained from Eq. (11) (blue line) is also plotted.

up to $O(|\Delta|^3)$.[7] Equation (2) is thereby transformed into

$$(-\lambda_{TF}^2 \boldsymbol{\nabla}^2 + 1)\boldsymbol{E} = \boldsymbol{B} \times \underline{R}_H \boldsymbol{j}, \tag{5}$$

where

$$\underline{R}_H \equiv \frac{1}{2eN(0)} \left\langle \frac{\partial \boldsymbol{v}_F}{\partial \boldsymbol{p}_F} \right\rangle_F \langle \boldsymbol{v}_F \boldsymbol{v}_F \rangle_F^{-1} \tag{6}$$

is the normal Hall coefficient. In particular, for a two-dimensional system with an isotropic Fermi surface, Eq. (5) can be rearranged into

$$(-\lambda_{TF}^2 \boldsymbol{\nabla}^2 + 1)\boldsymbol{E} = \frac{1}{2eN(0)\varepsilon_F} \boldsymbol{B} \times \boldsymbol{j}, \tag{7}$$

where ε_F is the Fermi energy of a two-dimensional free-electron model. We then substitute the expression for $\boldsymbol{j}$ near T_c[7] into Eq. (7) and assume the term with λ_{TF} ($\ll \xi_0$) to be negligible near T_c. Subsequently, we insert the resulting expression for $\boldsymbol{E}$ into Gauss' law $\rho(\boldsymbol{r}) = \epsilon_0 \boldsymbol{\nabla} \cdot \boldsymbol{E}$ and approximate $\boldsymbol{B}(\boldsymbol{r}) \approx \bar{\boldsymbol{B}}$ as appropriate near H_{c2}. We thereby obtain

$$\rho(\boldsymbol{r}) \simeq \frac{7\zeta(3)\hbar v_F^2 \epsilon_0}{32(\pi k_B T)^2 \varepsilon_F} \bar{B} \boldsymbol{\nabla}^2 |\Delta|^2, \tag{8}$$

where $\zeta(3) = 1.202\cdots$ is the Riemann zeta function. Now, the pair potential around the vortex core located at the origin may be approximated as

$$\Delta \simeq \Delta_{max} \sqrt{x^2 + y^2}/\xi_c, \tag{9a}$$

where ξ_c is the vortex core size and Δ_{max} denotes the maximum value of the pair potential in the vortex lattice. We may also express Δ_{max} on the basis of Abrikosov's theory[7,37] as

$$\Delta_{max} \simeq \alpha \Delta_0 \sqrt{\frac{B_{c2} - \bar{B}}{B_0}}, \tag{9b}$$

where

$$\alpha \equiv \sqrt{\frac{3^{\frac{1}{4}}}{4\left(1 - \frac{\xi_0^2}{4\lambda_L^2}\beta\right) I_{00}^{(4)}}}, \qquad B_0 \equiv \frac{\hbar}{2|e|\xi_0^2} \tag{9c}$$

with $\beta \equiv 7\zeta(3)\Delta_0^2/8(\pi k_B T)^2$ and $I_{00}^{(4)} = 1.16$. Substituting Eq. (9) into Eq. (8), we obtain

$$\rho(\mathbf{0}) \simeq \frac{\rho_0}{B_0^2} \frac{\alpha^2 \beta \delta}{(\xi_c/\xi_0)^2} \bar{B}(B_{c2} - \bar{B}). \tag{10}$$

Equation (10) with Eq. (9b) indicates that the magnetic field dependence of $\rho(\mathbf{0})$ is determined by the competition between the increasing magnetic field and the decreasing pair potential as $\rho(\mathbf{0}) \propto \bar{B}\Delta_{max}^2$. Although it was derived near T_c, Eq. (10) reproduces the key features of the field dependence of the core charge at low temperatures given in Fig. 3.

As already mentioned, alternative mechanisms for the core charging have been proposed by Khomskii and Freimuth[19] and Feigel'man and coworkers[20,21] based on considerations of an isolated vortex. Although different from each other in detail, the two mechanisms have a common feature that the reduction of $|\Delta(\mathbf{r})|$ in the presence of a finite slope in the

normal density of states is the key source for the vortex-core charging; they have little connection with the Lorentz force. Hence, charge accumulation in the core region by these mechanisms should decrease monotonically as H is increased. For example, the core charge density given by Khomskii and Freimuth[19] can also be expressed as

$$\rho_{\rm KF}/\rho_0 \simeq \delta\Delta_{\rm max}^2/\Delta_0^2 \sim O(\delta). \tag{11}$$

We also plot $\rho_{\rm KF}/\rho_0$ in Fig. 3, which is seen to decrease monotonically in marked contrast with the peak structure of $\rho(\mathbf{0})/\rho_0$. In other words, the Lorentz force mechanism for vortex-core charging can be experimentally distinguished from the other two mechanisms in an unambiguous manner by observing the magnetic-field dependence. Note also that the peak value of the charge density $\rho(\mathbf{0})$ is about 10 times larger than $\rho_{\rm KF}$ at $T/T_{\rm c} = 0.2$.

Next, we turn our attention to the $\lambda_{\rm L}$ dependence of vortex charging. Figure 4 plots the relative difference in the charge density at the vortex center between $\lambda_{\rm L} = 5\xi_0$ and $\lambda_{\rm L} = 20\xi_0$ at $T/T_{\rm c} = 0.5$, which we denote by $\delta\rho$, as a function of $\bar{B}/B_{\rm c2}$. Thus, $\delta\rho$ is of order 0.1 even at low fields and decreases rapidly as the field is increased, indicating that we can neglect the $\lambda_{\rm L}$ dependence of the charge density to the first approximation when considering it as a function of $\bar{B}/B_{\rm c2}$. In this context, it should be noted that charge accumulation due to the Lorentz force in *an isolated vortex* has a substantial $\lambda_{\rm L}$ dependence; indeed, $\delta\rho$ can be of order 1. This is because $\lambda_{\rm L}$ strongly affects the magnitude of $\boldsymbol{B}(\boldsymbol{r})$ around the core[7,37] and hence the core charge according to Eq. (2).

Finally, we estimate the order of the accumulated charge around a vortex from Eq. (10). Although derived near $T_{\rm c}$, we verified that the formula reproduces the numerical results in Fig. 3 reasonably well over $T \gtrsim 0.2T_{\rm c}$. Let us approximate the charge profile near the core center in Fig. 2 as a cone of radius $0.5\xi_0$ with the peak value in the simulation. We thereby obtain a rough estimate for the peak value of the accumulated charge $Q_{\rm unit}$ in the core region of radius $0.5\xi_0$ per length $\Delta z = 10$ Å along the flux line for $T/T_{\rm c} \lesssim 0.2$ as

$$Q_{\rm unit} \equiv \frac{\pi}{12}\Delta z\xi_0^2\rho(\mathbf{0})_{\rm max} \approx \pi\Delta z\xi_0^2\delta\rho_0 = \eta\delta\Delta_0|e|, \tag{12}$$

where $\eta \equiv \pi\epsilon_0\Delta z/|e|^2 \simeq 1.09\times10^{18}$ J^{-1}. For the metallic superconductor Nb, we adopt $k_{\rm F} \simeq 1.0$ Å, $\Delta_0 \simeq 1.4$ meV, and $\xi_0 \simeq 380$ Å[38] for Eq. (12) to obtain $Q_{\rm unit} \simeq 5\times10^{-7}|e|$ C. For the high-$T_{\rm c}$ superconductor $YBa_2Cu_3O_{7-x}$, we may substitute $k_{\rm F} \simeq 1.0$ Å, $\Delta_0 \simeq 28$ meV,[39] and $\xi_0 \simeq 30$ Å[40] into Eq. (12), thereby obtaining $Q_{\rm unit} \simeq 1\times10^{-4}|e|$ C. As can be seen from Eq. (12), δ and Δ_0 are crucial elements determining the magnitude of the accumulated charge. In this context, the parameter δ of the iron-based layered superconductor FeSe has been reported to reach as high as $\delta \sim 1$.[41] Hence, we now have a greater chance of clearly observing the field dependence. Among the possible experimental methods to this end are nuclear magnetic resonance[40,42] and the Kelvin method for measuring the Hall voltage.[13,14] Finally, it should be noted that the Fermi surface curvature is another crucial element determining the magnitude and sign of the vortex-core charge.[9,10]

In summary, we have clarified the magnetic field dependence of the vortex-core charge due to the Hall effect using augmented quasiclassical equations of superconductivity both numerically and analytically. We found a peak structure characteristic of the Lorentz force mechanism for charging that should be common among all type-II superconductors. Its observation to confirm the Lorentz force on persistent currents is a challenging topic.

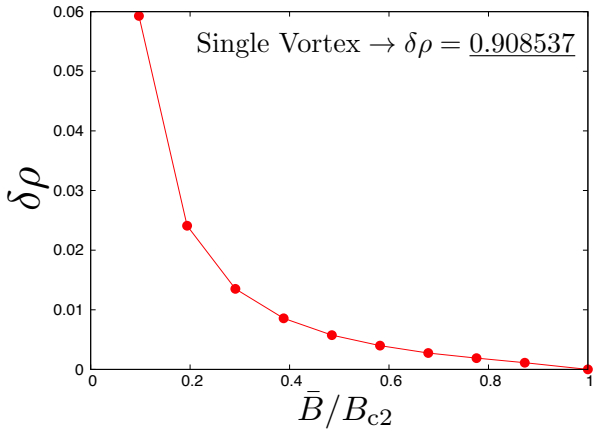

Fig. 4. (Color online) Relative difference in the charge density at the vortex center between $\lambda_{\rm L} = 5\xi_0$ [$\equiv \rho(\mathbf{0})_5$] and $\lambda_{\rm L} = 20\xi_0$ [$\equiv \rho(\mathbf{0})_{20}$], where $\delta\rho$ is defined as $[\rho(\mathbf{0})_5 - \rho(\mathbf{0})_{20}]/\rho(\mathbf{0})_5$.

1) E. H. Hall, Am. J. Math. **2**, 287 (1879).
2) See, for example, R. E. Prange and S. M. Girvin (eds.), *The Quantum Hall Effect* (Springer, New York, 1990).
3) V. L. Ginzburg and L. D. Landau, Zh. Eksp. Teor. Fiz **20**, 1064 (1950).
4) G. Eilenberger, Z. Phys. **214**, 195 (1968).
5) R. D. Parks (ed.), *Superconductivity* (Marcel Dekker, New York, 1969).
6) N. B. Kopnin, *Theory of Nonequilibrium Superconductivity* (Oxford University Press, New York, 2001).
7) T. Kita, *Statistical Mechanics of Superconductivity* (Springer, Tokyo, 2015).
8) T. Kita, Phys. Rev. B **64**, 054503 (2001).
9) H. Ueki, W. Kohno, and T. Kita, J. Phys. Soc. Jpn. **85**, 064702 (2016).
10) T. Kita, Phys. Rev. B **79**, 024521 (2009).
11) A. G. van Vijfeijken and F. A. Staas, Phys. Lett. **12**, 175 (1964).
12) C. J. Adkins and J. R. Waldram, Phys. Rev. Lett. **21**, 76 (1968).
13) J. Bok and J. Klein, Phys. Rev. Lett. **20**, 660 (1968).
14) T. D. Morris and J. B. Brown, Physica (Amsterdam) **55**, 760 (1971).
15) N. B. Kopnin and V. E. Kravtsov, Zh. Eksp. Teor. Phys. **23**, 631 (1976) [Sov. Phys. JETP **23**, 578 (1971)].
16) E. Arahata and Y. Kato, J. Low. Temp. Phys. **175**, 346 (2014).
17) For an experimental overview and references, see, for example, S. J. Hagen, A. W. Smith, M. Rajeswari, J. L. Peng, Z. Y. Li, R. L. Greene, S. N. Mao, X. X. Xi, S. Bhattacharya, Q. Li, and C. J. Lobb, Phys. Rev. B **47**, 1064 (1993).
18) T. Nagaoka, Y. Matsuda, H. Obara, A. Sawa, T. Terashima, I. Chong, M. Takano, and M. Suzuki, Phys. Rev. Lett. **80**, 3594 (1998).
19) D. I. Khomskii and A. Freimuth, Phys. Rev. Lett. **75**, 1384 (1995).
20) M. Feigel'man, V. Geshkenbein, A. Larkin, and V. M. Vinokur, JETP Lett. **62**, 834 (1995).
21) G. Blatter, M. Feigel'man, V. Geshkenbein, A. Larkin, and A. Otterlo,

Phys. Rev. Lett. **77**, 566 (1996).
22) N. Hayashi, M. Ichioka, and K. Machida, J. Phys. Soc. Jpn. **67**, 3368 (1998).
23) M. Matsumoto and R. Heeb, Phys. Rev. B **65**, 014504 (2001).
24) Y. Chen, Z. D. Wang, J. X. Zhu, and C. S. Ting, Phys. Rev. Lett. **89**, 217001 (2002).
25) D. Knapp, C. Kallin, A. Ghosal, and S. Mansour, Phys. Rev. B **71**, 064504 (2005).
26) J. W. Serene and D. Rainer, Phys. Rep. **101**, 221 (1983).
27) A. I. Larkin and Y. N. Ovchinnikov, in *Nonequilibrium Superconductivity*, ed. D. N. Langenberg and A. I. Larkin (Elsevier, Amsterdam, 1986) Vol. 12, p. 493.
28) T. Kita, J. Phys. Soc. Jpn. **67**, 2067 (1998).
29) M. Ichioka, N. Hayashi, N. Enomoto, and K. Machida, Phys. Rev. B **53**, 15316 (1996).
30) U. Klein, J. Low Temp. Phys. **69**, 1 (1987).
31) Y. Nagato, K. Nagai, and J. Hara, J. Low Temp. Phys. **93**, 33 (1993).
32) N. Schopohl and K. Maki, Phys. Rev. B **52**, 490 (1995).
33) E. Helfand and N. R. Werthamer, Phys. Rev. Lett. **13**, 686 (1964).
34) T. Kita and M. Arai, Phys. Rev. B **70**, 224522 (2004).
35) M. Ichioka, A. Hasegawa, and K. Machida, Phys. Rev. B **59**, 8902 (1999).
36) W. H. Press, S. A. Teukolsky, W. T. Vetterling, and B. P. Flannery, *Numerical Recipes: The Art of Scientific Computing* (Cambridge Univ. Press, Cambridge, 2007) 3rd ed.
37) A. A. Abrikosov, Zh. Eksp. Teor. Fiz. **32**, 1442 (1957) [Sov. Phys. JETP **5**, 1174 (1957)].
38) O. Klein, E. J. Nicol, K. Holczer, and G. Grüner, Phys. Rev. B **50**, 6307 (1994).
39) H. L. Edwards, J. T. Markert, and A. L. de Lozanne, Phys. Rev. Lett. **69**, 2967 (1992).
40) K. Kumagai, K. Nozaki, and Y. Matsuda, Phys. Rev. B **63**, 144502 (2001).
41) S. Kasahara, T. Watashige, T. Hanaguri, Y. Kohsaka, T. Yamashita, Y. Shimoyama, Y. Mizukami, R. Endo, H. Ikeda, K. Aoyama, T. Terashima, S. Uji, T. Wolf, H. von Löhneysen, T. Shibauchi, and Y. Matsuda, Proc. Natl. Acad. Sci. U.S.A. **111**, 16309 (2014).
42) A. M. Mounce, S. Oh, S. Mukhopadhyay, W. P. Halperin, A. P. Reyes, P. Kuhns, K. Fujita, M. Ishikado, and S. Uchida, Nat. Phys. **7**, 125 (2011).